Supplementary Information

Surface-dependence of defect chemistry of nano-structured ceria

S. Agarwal, [a] *X. Zhu,* [b] *E. J. M. Hensen,* [b] *B. L. Mojet,* [a] *L. Lefferts* [a,c]*

[a] Catalytic Processes and Materials, MESA+ Institute for Nanotechnology, Faculty of Science and Technology, University of Twente, PO Box 217, 7500 AE Enschede, The Netherlands

[b] Schuit Institute of Catalysis, Laboratory of Inorganic Materials Chemistry, Department of Chemical Engineering and Chemistry, Eindhoven University of Technology, PO Box 513, 5600 MB Eindhoven, The Netherlands

[c] Aalto University, School of Chemical Technology, Department of Biotechnology and Chemical Technology, Research Group Industrial Chemistry, P.O. Box 16100, FI-00076 Aalto, Finland.

In figure S1, *in-situ* Raman raw and smoothened spectra for octahedron and cube samples obtained in He and 33 vol% CO/He gas flow stream respectively are shown. All the Raman spectra shown in the present paper are smoothened (25 points) to better define any observed changes introduced on exposure to CO/H_2O. As evident from figure S1, the CO-induced changes observed in smoothened spectrum are real and not the artefact of data smoothing.

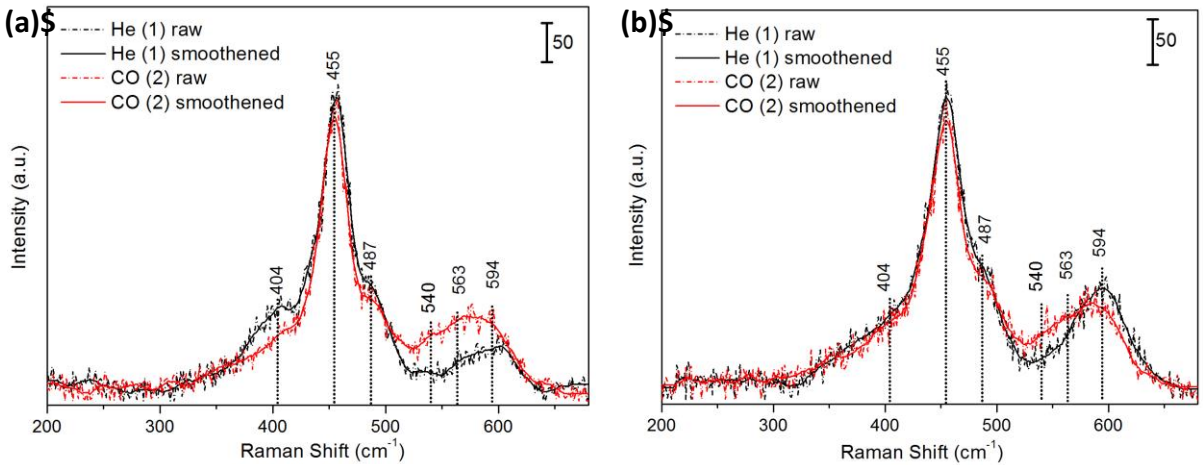

Figure S1. *In-situ* Raman raw (dash-dotted) vs. smoothened (solid) spectra of ceria (a) octahedron and (b) cube in He (black) and 33 vol% CO/He (red) flow at 350°C.

The normalized Raman and FTIR plots of ceria nanoshapes at 350^{o}C are shown in figure S2. These spectra are obtained for ceria nanoshapes that were not pretreated with H_2.

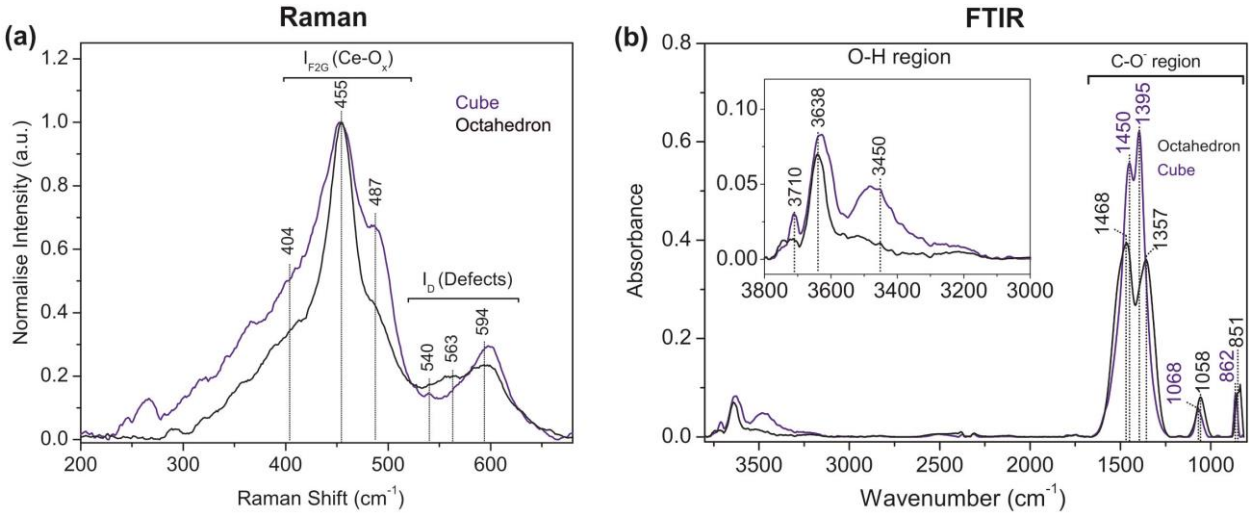

Figure S2. *In-situ* normalized Raman (a) and FTIR (b) spectra of unreduced ceria octahedron (black) and cube (blue) in He flow at 350^{o}C.

The Raman spectra of unreduced ceria nanoshapes obtained on exposure to CO are shown in figure S3. The ceria samples used for investigation did not undergo any prior H_2 pretreatment.

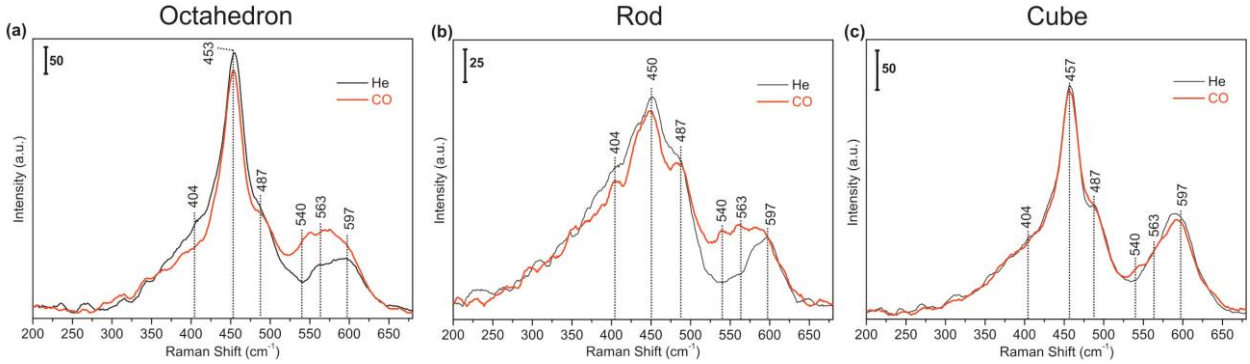

Figure S3: In-situ Raman spectra of unreduced ceria (a) octahedra, (b) rod and (c) cube at 350^{o}C obtained in He (black) flow followed by CO (red) flow.

FTIR spectra of H_2-reduced ceria octahedra at 350^{o}C are shown in figure S4. On introduction of CO, –OH^{3640} slightly increase in intensity with decrease in intensity of –OH^{3668} and the broad –OH band in region 3500-3000 cm^{-1} (Figure S4a). Peaks related to C-H stretch of formate species at 2945 and 2838cm^{-1} were observed. In addition, peaks at 1580, 1457, 1388, 1298, 1055 and 854 cm^{-1} were also observed. These peaks are related to C-O^- stretching and bending vibration of carbonate and formate species. In He after CO, subtle increase in intensity of –OH^{3668} peaks was observed (figure S4b). Formate species (evident from 2945 and 2838 cm^{-1} peaks) disappeared. Band in region 1800-1200 cm^{-1} were less broad due to the disappearance of peak at 1580cm^{-1}. Peaks at 1055 and 854 cm^{-1} slightly decreased in intensities. Subsequently in H_2O, an increase in intensity of –OH peaks were observed. Broad –OH band in region 3500-3000 cm^{-1} increased in intensity. For further details see subtracted section (figure 4). Bands related to carbonate species partly decomposed in presence of H_2O. Please note that all the carbonates formed in presence of CO does not disappeared indicating the formation of stable carbonates. Finally in He after H_2O, the decrease in intensity of –OH peaks were observed (figure S4d). Broad –OH band in region 3500-3000 cm^{-1} decreased in intensity due to desorption of physisorbed water. Bands related to carbonate species showed an increase in intensity at 1457 and 1388 cm^{-1} with the decrease in 1553 and 1530 cm^{-1} band. This is suggested to be due to the re-structuring of carbonates on octahdera, as well as the change in dipole moment of C-O bond caused due to the removal of weakly adsorbed water.

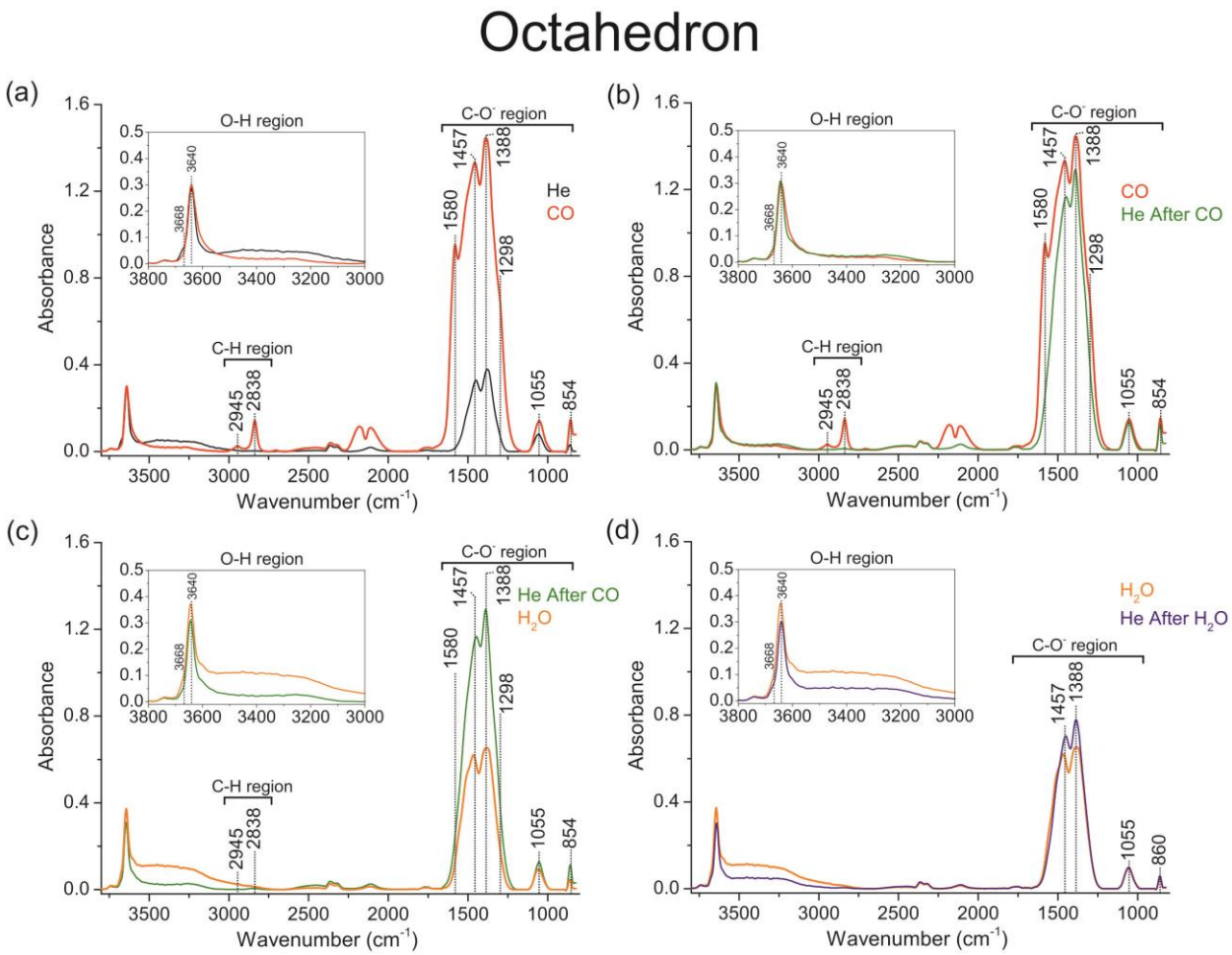

Figure S4: *In-situ* FTIR spectra at 350°C of reduced ceria octahedra in a) He (1), followed by CO (2); b) CO (2) - He (1) spectrum; c) CO (2) followed by He (3); d) He (3) - CO (2) spectrum; e) He (3) followed by H_2O/He (4); f) H_2O (4) - He (3) spectrum; g) in H_2O (4) followed by He (5); h) He (5) - H_2O (4) spectrum.

In Figure S5, the FTIR spectra of ceria rods obtained in different gas treatments are shown. As the observation for rods are similar to octahedra, refer to the description of the previous figure S4 for details.

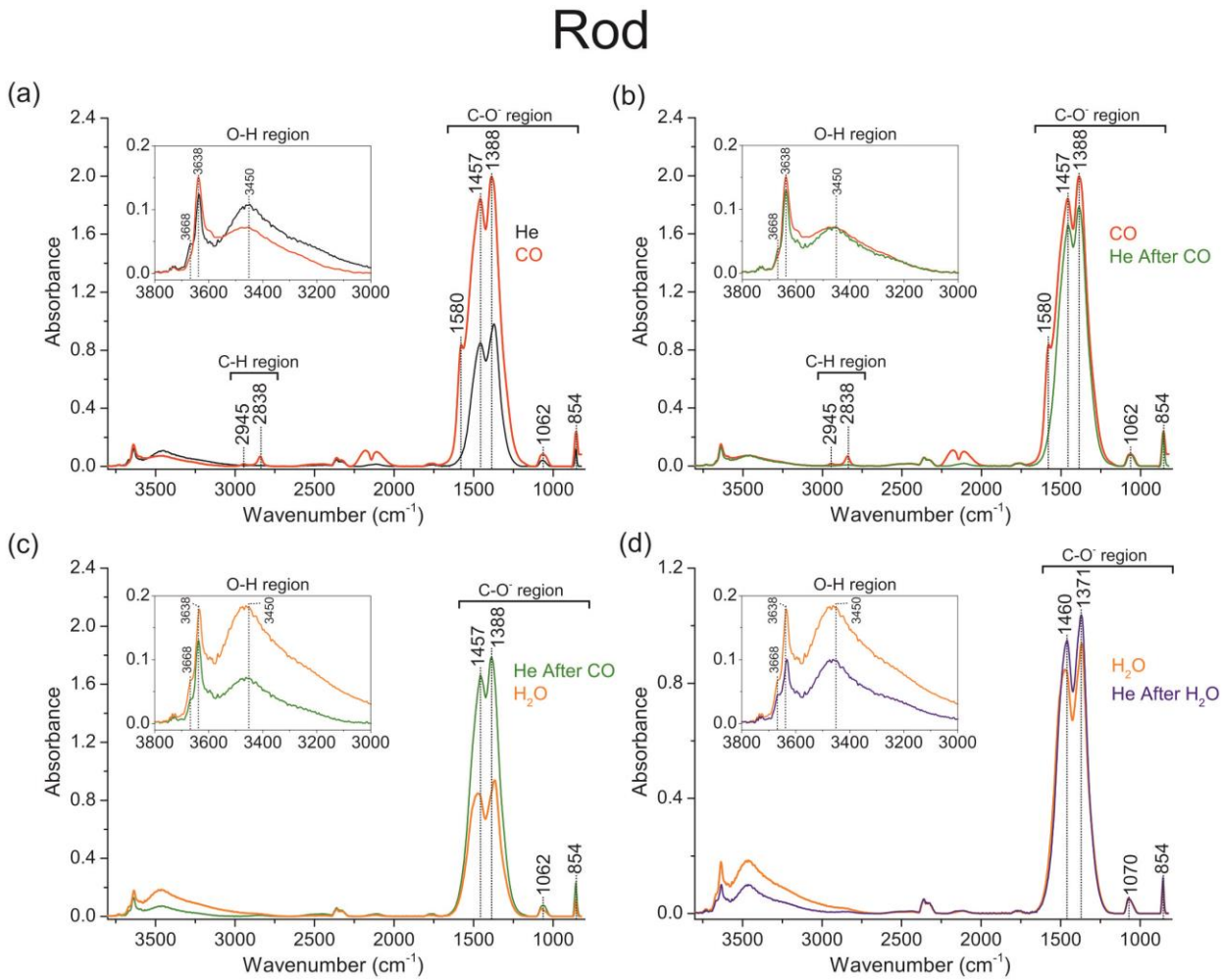

Figure S5: *In-situ* FTIR spectra at 350°C of reduced ceria rods in a) He (1), followed by CO (2); b) CO (2) - He (1) spectrum; c) CO (2) followed by He (3); d) He (3) - CO (2) spectrum; e) He (3) followed by H_2O/He (4); f) H_2O (4) - He (3) spectrum; g) in H_2O (4) followed by He (5); h) He (5) - H_2O (4) spectrum.

The resulting FTIR spectra of cubes obtained on exposure to CO and H_2O are shown in figure S6. In CO, significant amount of carbonates and formates were formed (figure S6a). Formate formation was evident from the peaks at 2845 and 1580 cm^{-1}, whereas C-O stretch of carbonates were observed at 1391 and 866 cm^{-1}. Furthermore, $–OH^{3602}$ increased in intensity with decrease in intensity of $–OH^{3670}$ and a broad –OH band in region 3500-3000 cm^{-1}.

Upon exposure to He, subtle increase in intensity of $–OH^{3670}$ peak was observed (figure S6b). For further details see subtracted section (figure 4). Likewise octahedra and rods, 2945 and 2845 cm^{-1} peaks related to C-H stretch of formats disappeared. Bands in the region 1800-1200 cm^{-1} were less broad due to the disappearance of peak at 1580 cm^{-1}. Peaks at 1069 and 866 cm^{-1} decreased in intensities.

On introduction of H_2O vapor, increase in intensity of –OH peaks were observed along with increase in broad –OH band in the region 3500-3000 cm^{-1}. Bands related to carbonate species decomposed in presence of H_2O.

Finally in He after H_2O, overall decrease in intensity of –OH peaks was observed (figure S6d). Due to desorption of physisorbed water, broad –OH band in the region 3500-3000 cm^{-1} further decreased in intensity. Bands related to carbonate species showed an increase in intensity at 1470 and 1391 cm^{-1} with a subtle decrease in 1553 and 1530 cm^{-1} peaks. Unlike octahedra and rods, we suggest that the change in dipole moment is the dominating factor influencing the intensity of C-O peaks.

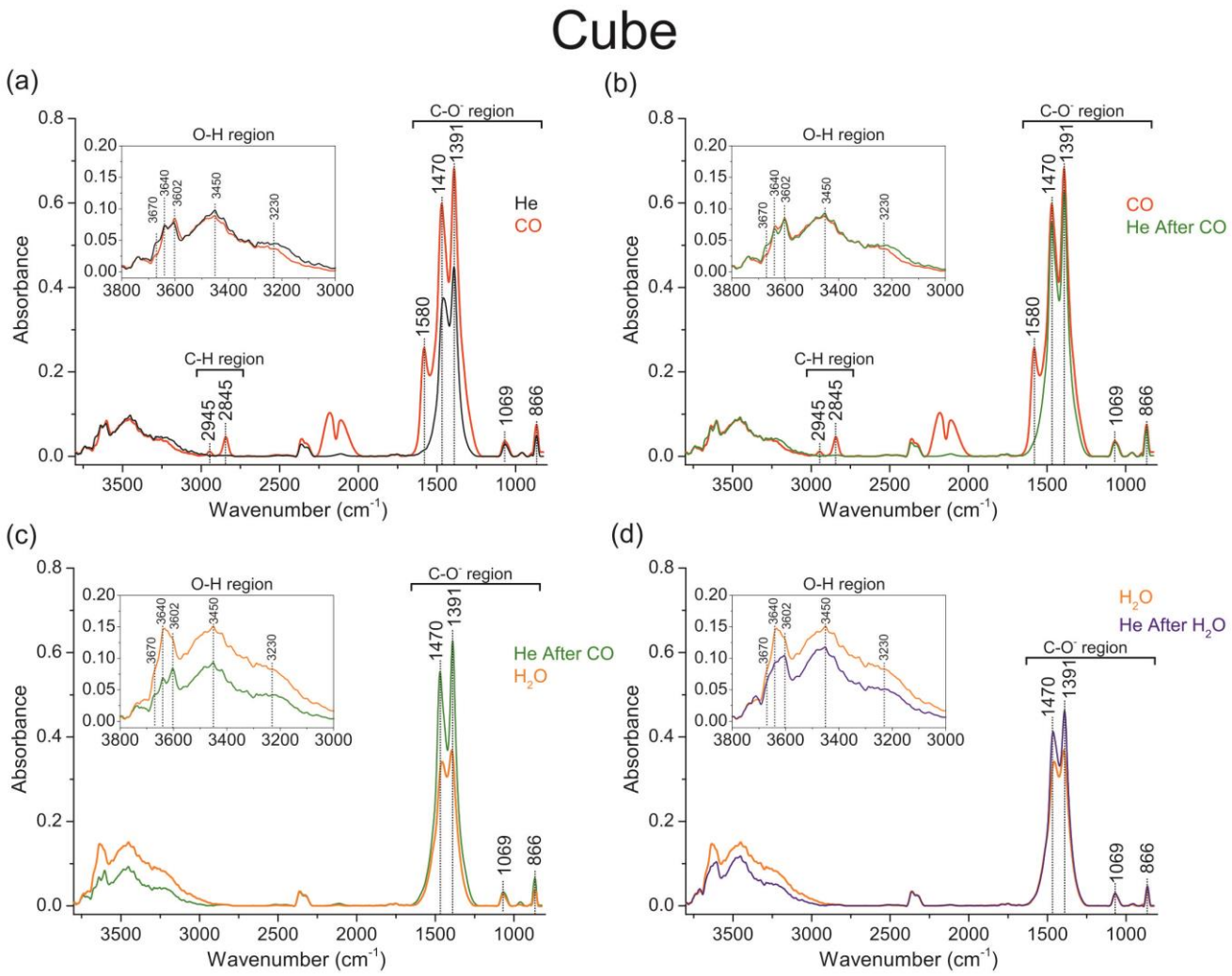

Figure S6: *In-situ* FTIR spectra at 350°C of reduced ceria cubes in a) He (1), followed by CO (2); b) CO (2) - He (1) spectrum; c) CO (2) followed by He (3); d) He (3) - CO (2) spectrum; e) He (3) followed by H_2O/He (4); f) H_2O (4) - He (3) spectrum; g) in H_2O (4) followed by He (5); h) He (5) - H_2O (4) spectrum.

In figure S7, Raman spectra of ceria rods obtained in consecutive gas treatments are shown. As can be seen in figure S7a, the fluorite peaks (404, 455 and 487 cm^{-1}) decreases in intensity and new defects (540, 563, 594 cm^{-1}) are created on introduction of CO. Subsequently on flowing He after CO, subtle changes in the fluorite (350-500 cm^{-1}) and defect (500-600 cm^{-1}) region were observed. On exposure to H_2O/He, fluorite peaks further increased in intensity with major disappearance of defect bands. Finally in He after H_2O, further increase in fluorite peaks observed and the remaining CO-induced defects disappeared. The Raman behavior for rods is similar to the octahedra, indicating that defect chemistry is dependent on the exposed planes.

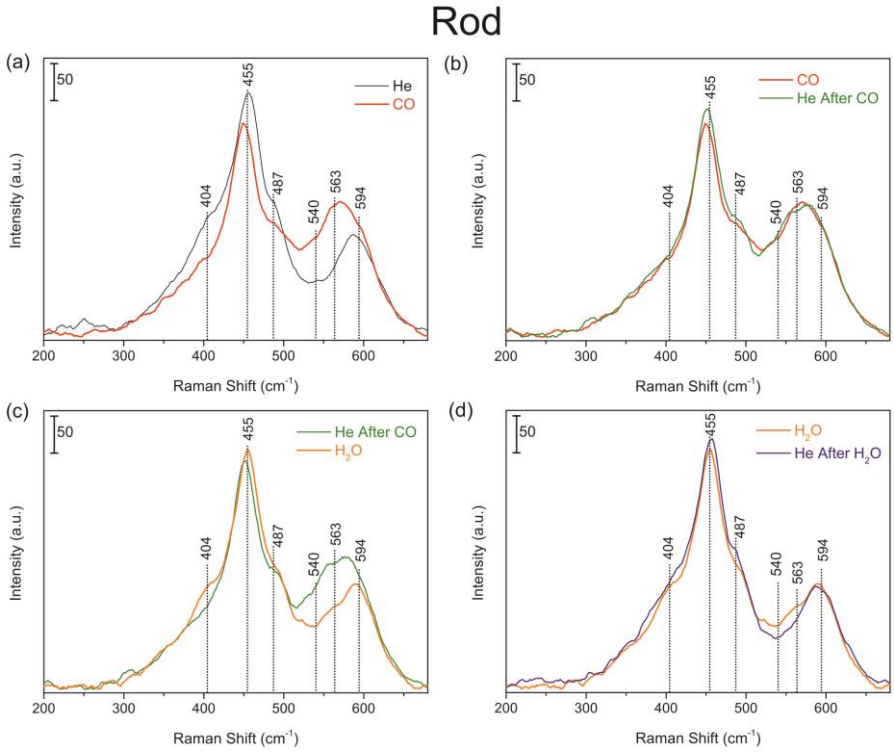

Figure S7: In-situ Raman spectra at 350^{o}C of reduced ceria rod in; (a) He (1), followed by CO (2); (b) CO (2) followed by He (3); (c) He (3) followed by H_2O/He (4); (d) H_2O/He followed by He (5) flow.

In Figure S8, the subtracted FTIR spectra of ceria rods obatined by subtracting the spectrum in 'before' and 'after' stage can be seen. The observations for rods are similar to octahedra, therefore for detailed description refer to the main paper (FTIR section for octahedra).

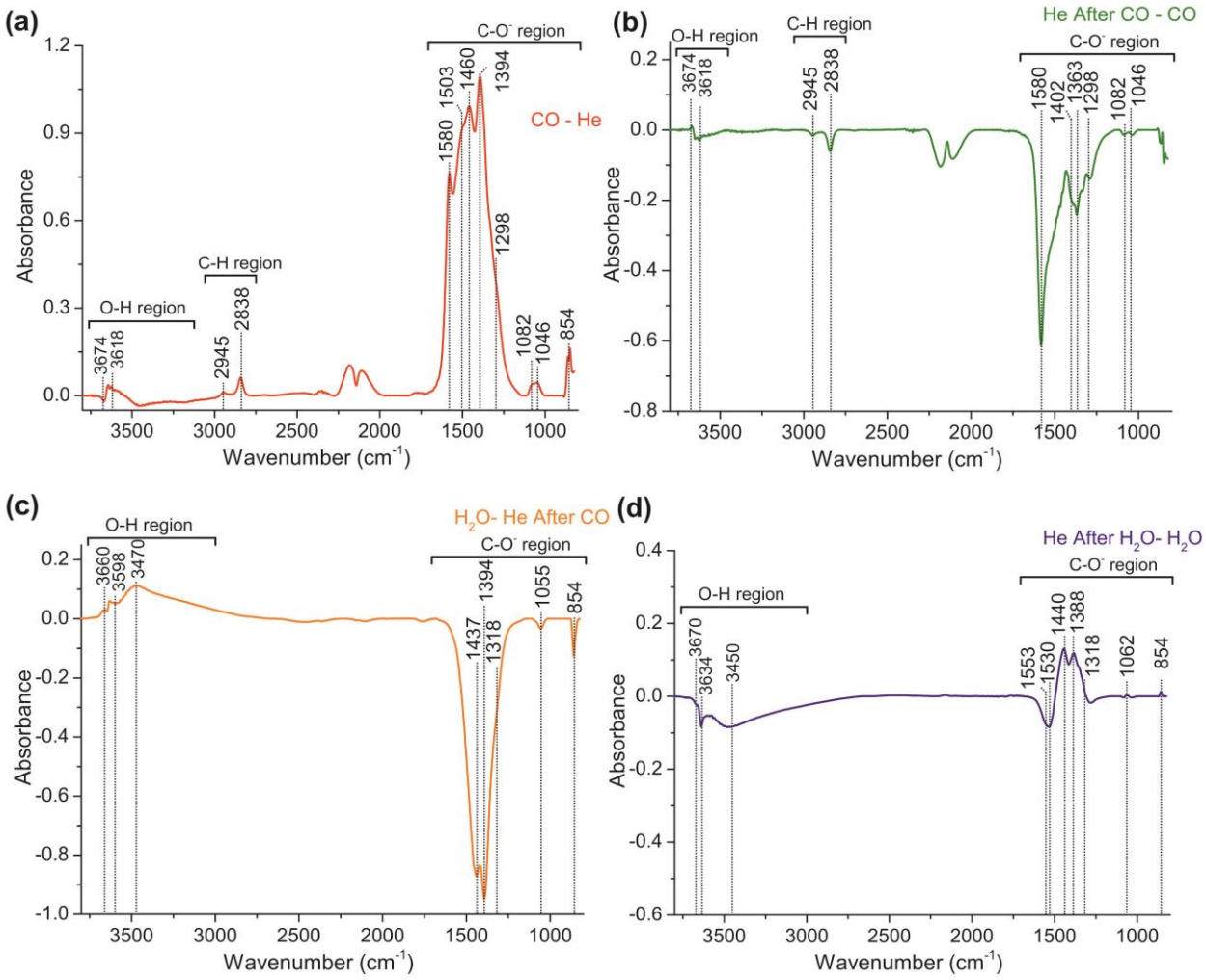

Figure S8. In-situ FTIR spectrum of reduced ceria rods at 350°C obtained by subtracting (a) He (1) from CO (2); (b) CO (2) from He (3); (c) He (3) from H_2O (4); (d) H_2O (4) from He (5) spectrum. Inset in figure S7d are expanded spectra of carbonate regions obtained in H_2O (dash-dotted orange) and He (5, blue) flow.

In figure S9, the FTIR spectra for ceria nanorods obtained after exposure to CO and H_2O can be seen. The observations for rods is similar to octahedra (figure 5a). For details refer to result section (*In-situ* FTIR: CO adsorption on Ce^{4+} and Ce^{3+}).

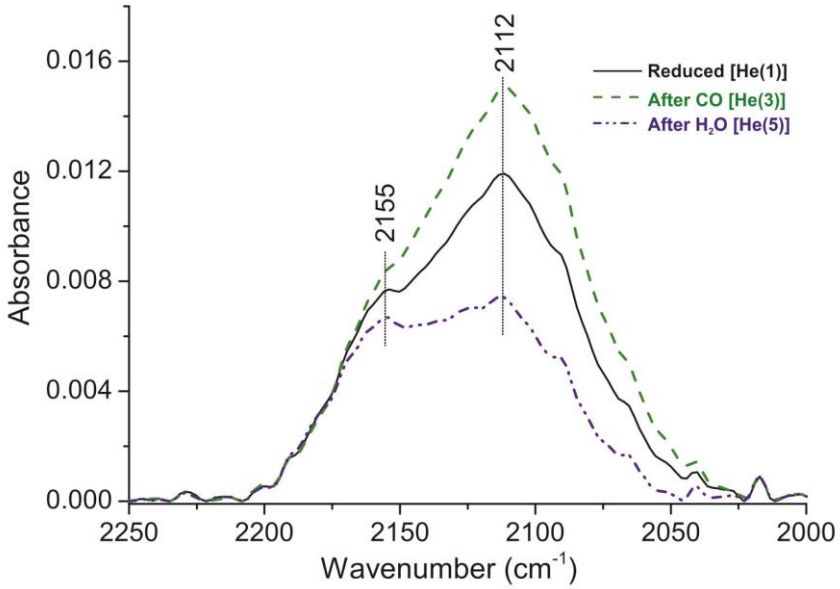

Figure S9. In-situ FTIR of reduced ceria rod at 350^{o}C obtained in He (1), He (3) and He (5) flow. Key: He (1) black solid line, He (3) dashed green line and He (5) dash-dotted blue line.

Subtracted Raman spectra of ceria rods obtained at 350°C are shown in figure S10. In the resulted spectrum the changes occurred on introduction of CO (red) and H_2O (blue) can be seen. On comparing with octahedra (figure 6a), it is apparent that the CO/H_2O induced changes for both shapes is similar.

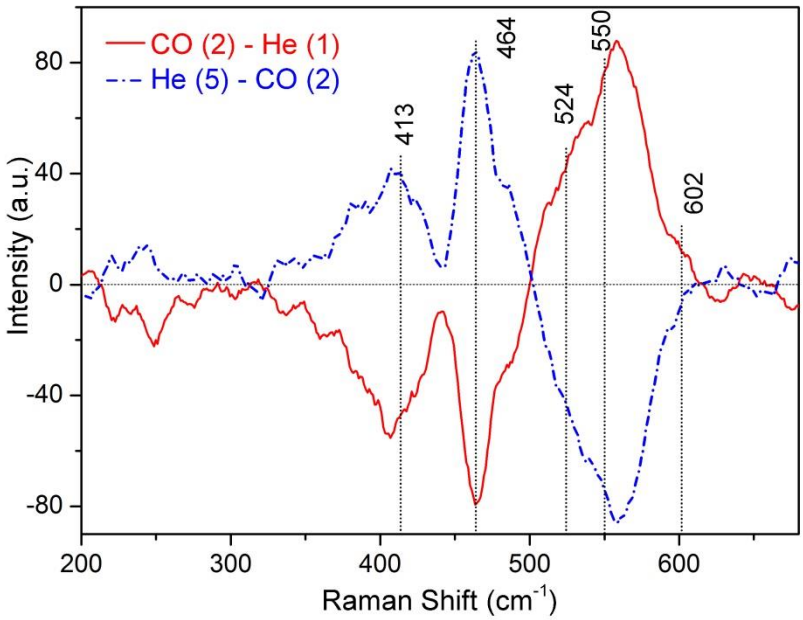

Figure S10. Subtracted Raman spectra of reduced ceria rod obtained at 350°C. Red spectrum is the spectrum obtained by subtracting He (1) with CO (2). Blue spectrum is the CO (2) subtracted with He (5).

The lattice representations (side view) of the (111) and (100) ceria surfaces are shown in figure S11. The CeO_2 (111) surface has both Ce and O accessible in the top layer, whereas CeO_2 (100) has either O or Ce accessible in top layer.

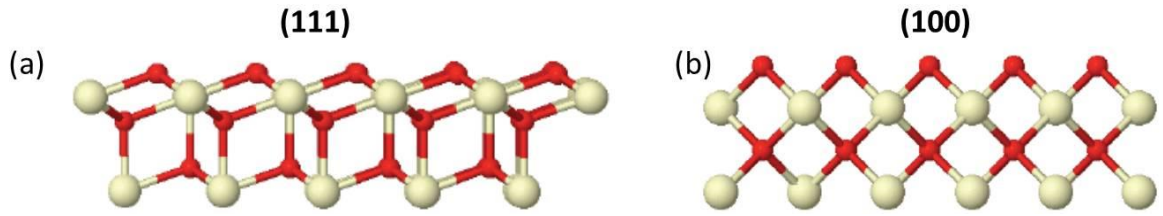

Figure S11. The ball and stick model of the (111) and (100) surfaces. Key: Ce (Light yellow) and O (red) atoms. These structures were drawn using Jmol (an open-source Java viewer for chemical structures in 3D; http://www.jmol.org/).

The effect of pretreatment on ceria octahedron is shown in figure S12. As can be seen in figure S12, the CO adsorbed peak on Ce^{3+} site is observed at 2112 cm^{-1} for the reduced ceria sample. This featured peak is not observed for the octahedron sample pretreated in oxygen.

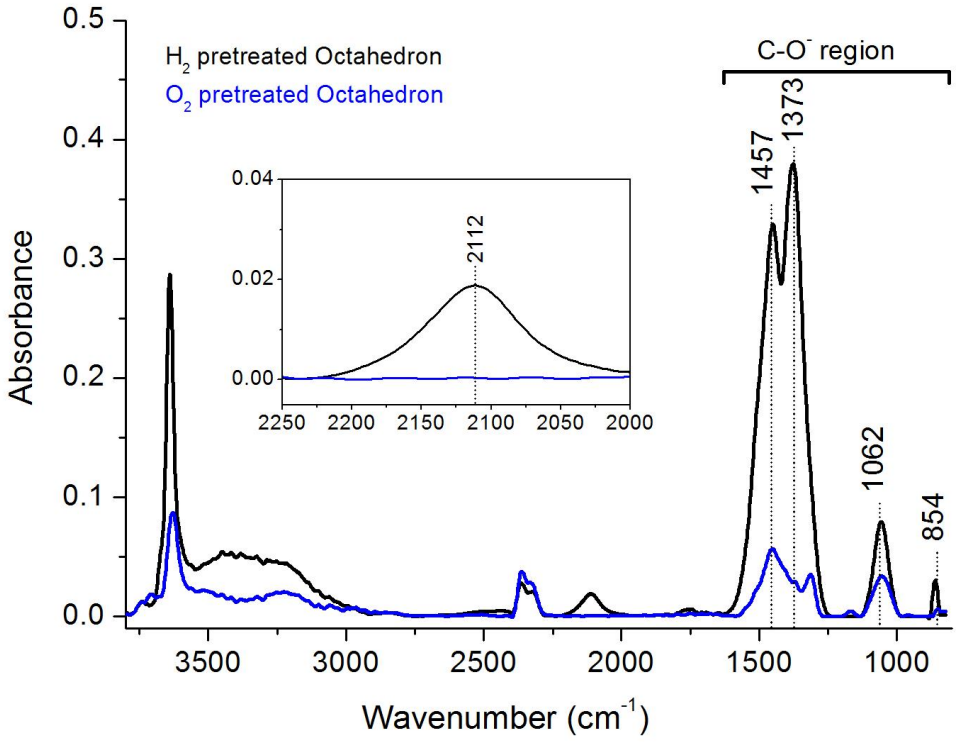

Figure S12. *In-situ* FTIR spectra of reduced (black) and oxidized (blue) ceria octahedra in He at 350^{o}C.

Pressing details

The two experimental techniques (FTIR and Raman) require slightly different sample preparations in terms of the amount of applied pressure to press the samples, whilst it is known that rare-Earth oxides undergo pressure-induced phase transformations. Specifically, for the IR technique we apply ~2 tons of force to obtain an 8 mm self-supporting pellet (applied pressure ~0.4 GPa), whilst the Raman technique uses a much lower (hand applied) pressure to obtain a packed bed (estimated applied pressure ~10^{-4} GPa).

It must be noted that bulk ceria undergoes a phase transformation at a pressure of 31 GPa. [1] This is irreversible down to 11 GPa but fully reversible below this. On the nanoscale the onset of this phase transformation reduces to a pressure of 22.3 GPa for ~10 nm particles. [2] We never apply more than 0.4 GPa in our experiments; therefore we never induce such a phase transformation in our samples. Furthermore, even if we had induced the phase transformation, our experiments are carried out at atmospheric pressure whereupon the phase transformation would have reversed.

Now we have established that our sample does not undergo a pressure-induced phase transformation, it is interesting to calculate the geometric changes in the sample due to the application of the small amount of pressure during our sample preparation. Ceria obeys a first-order Birch equation of state with fitting parameters B_0=230 GPa and B_0'=4. [3] The volumetric change due to 0.4 GPa of applied pressure is then found to be only 0.13 %.

We expect such a small volumetric change to have little or no effect on our sample spectra and we further demonstrate this be calculating the F_{2g} peak shift due to a pressure change of 0.4 GPa. Kourouklis *et al.* measured the frequency shift-pressure relation to be $d\omega/dP$~3.29 cm^{-1}/GPa. [1] From this we calculate the frequency-shift in our experiments to be 1.3 cm^{-1}, which is below our resolution of 2 cm^{-1}.

To summarize:

1. We are not applying enough pressure to induce a phase transformation and, even if we were, we conduct the experiments at atmospheric pressure and the transformations are reversible below 11 GPa.
2. Our samples for the IR experiments are expected to change by only 0.13 % in volume during sample pressing but, again, we expect this to be reversible when releasing the pressure prior to experimentation.
3. The expected frequency shift for F_{2g} peak due to the applied pressure is below our resolution limit.
4. We are reporting changes due to the introduction of different gases. The differences we see are due to different gas types, not different pressures.